

# Does the LHC exclude SUSY Particles at the ILC? \*

A. BHARUCHA<sup>1†</sup>, S. HEINEMEYER<sup>2‡</sup>, F. VON DER PAHLEN<sup>2,3§¶</sup>

<sup>1</sup> *Physik Department T31, Technische Universität München, James-Franck-Straße 1,  
D-85748 Garching, Germany*

<sup>2</sup> *Instituto de Física de Cantabria (CSIC-UC), E-39005 Santander, Spain*

<sup>3</sup> *Instituto de Física, Universidad de Antioquia, Calle 70 No. 52-21, Medellín, Colombia*

## Abstract

No.

arXiv:1404.0365v1 [hep-ph] 1 Apr 2014

---

\*Talk presented by S.H. at the International Workshop on Future Linear Colliders (LCWS13), Tokyo, Japan, 11-15 November 2013.

†email: Aoife.Bharucha@tum.de

‡email: Sven.Heinemeyer@cern.ch

§email: fp@gfif.udea.edu.co

¶MultiDark Fellow

# 1 Introduction

The LHC is actively searching for physics beyond the Standard Model (BSM), where the Minimal Supersymmetric Standard Model (MSSM) [1] is one of the leading candidates. The search for supersymmetry (SUSY) at the LHC has not (yet) led to a positive result. In particular, bounds on the first and second generation squarks and the gluinos from ATLAS and CMS are very roughly at the TeV scale, depending on details of the assumed parameters, see e.g. [2]. On the other hand, bounds on the electroweak SUSY sector, where  $\tilde{\chi}_{1,2}^{\pm}$  and  $\tilde{\chi}_{1,2,3,4}^0$  denote the charginos and neutralinos (i.e. the charged and neutral SUSY partners of the SM gauge and Higgs bosons) are substantially weaker.

There are several good motivations to expect electroweak SUSY particles with masses around a few hundred GeV.

- Models based on Grand Unified Theories (GUTs) naturally predict a lighter electroweak spectrum (see Ref. [3] and references therein).
- The anomalous magnetic moment of the muon shows a more than  $\sim 4\sigma$ , deviation from the SM prediction, see Ref. [4] and references therein. Agreement of this measurement with the MSSM requires charginos and neutralinos in the range of several hundreds of GeV.
- Charginos and neutralinos in the few hundred GeV range (possibly together with not too heavy scalar leptons) could easily bring the prediction of the  $W$  boson mass in full agreement with experimental data, see Ref. [5] and references therein.
- On the more speculative side, light charginos and neutralinos could also explain the small discrepancies in the  $pp \rightarrow W^+W^- + X$  measurements visible in all published data from ATLAS and CMS, see Ref. [6] and references therein.

These points provide a strong motivation for the search of these electroweak particles, which could be in the kinematic reach of the LHC. ATLAS [7–12] and CMS [13, 14] are actively searching for the direct production of charginos and neutralinos, in particular for the process  $pp \rightarrow \tilde{\chi}_1^{\pm}\tilde{\chi}_2^0$  with the subsequent decays  $\tilde{\chi}_1^{\pm} \rightarrow \tilde{\chi}_1^0W^{\pm}$  and  $\tilde{\chi}_2^0 \rightarrow \tilde{\chi}_1^0Z$ , resulting a three lepton signature. These searches are performed mostly in so-called “simplified models”, where the branching ratios of the relevant SUSY particles are set to one, assuming that all other potential decay modes are kinematically forbidden.

Based on those (and similar) analyses strong claims about excluded mass regions, e.g. in the  $m_{\tilde{\chi}_2^0}-m_{\tilde{\chi}_1^0}$  plane are made. This kind of bounds apparently exclude to a large extent the production of light charginos and/or neutralinos at the  $e^+e^-$  International Linear Collider (ILC), which is expected to operate with a center-of-mass energy of  $\sqrt{s} \leq 1$  TeV. On the other hand, if the charginos and neutralinos were to lie within reach of the ILC, it should be possible to reconstruct some or all of the fundamental parameters describing the electroweak sector of the MSSM (see e.g. [15]). Here we briefly review LHC exclusion bounds on electroweak particles, in particular in the  $\tilde{\chi}_1^{\pm}\tilde{\chi}_2^0$  search, and their “correct” interpretation as exclusions bounds [16].<sup>1</sup>

---

<sup>1</sup> We will not discuss LHC bounds on colored particles, which often appear to be strong, but where it is crucial to keep in mind the assumptions made to obtain these bounds.

## 2 What does the LHC (really) exclude?

In the case that the coloured sector is heavy, the direct production of charginos and neutralinos might provide the largest cross-sections of SUSY particles at the LHC. The golden channel for SUSY production is of chargino neutralino ( $\tilde{\chi}_1^\pm \tilde{\chi}_2^0$ ) pair production, dominated by the  $s$ -channel  $W$  boson mode. In the absence of light sleptons, the  $\tilde{\chi}_1^\pm$  decays via  $W^\pm \tilde{\chi}_1^0$ , while the  $\tilde{\chi}_2^0$  may decay either to a Higgs or a  $Z$  boson, and a  $\tilde{\chi}_1^0$ .

However, the experimental results for these decay channels are usually interpreted in terms of a simplified model which assumes 100% branching fraction to the  $Z$ , an assumption which leads to an incorrect interpretation once the decay to the Higgs boson is open. Here we review the analysis of the effect on the exclusion limits when the branching ratio to the Higgs is included. We will first define our notation and discuss the details of the calculation, then discuss simplified expressions for the couplings relevant for the  $\tilde{\chi}_2^0$  decays, and finally present some results for the reinterpreted limits, considering both the dependence on  $\tan\beta$  (the ratio of the two vacuum expectation values of the two MSSM Higgs doublets) and the phase of the  $U(1)$  gaugino mass parameter,  $\varphi_{M_1}$ .

### 2.1 Details of the calculation

The parameters entering the chargino–neutralino sector are the bino mass  $M_1$ , the wino mass  $M_2$ , the higgsino mass  $\mu$  as well as  $\tan\beta$ , and  $c_w = M_W/M_Z$  and  $s_w = \sqrt{1 - c_w^2}$  where  $M_Z$  is the mass of the  $Z$  boson. When working in the complex MSSM the parameters  $M_1$ ,  $M_2$  and  $\mu$  can in principle have a non-zero complex phase. However, one of the phases of these parameters, here  $\varphi_{M_2}$ , can be rotated away, in which case the phase  $\varphi_\mu$  is tightly constrained [17]. Therefore we take  $\mu$  to be a real parameter. Further note that in the case of the complex MSSM, the three neutral Higgs bosons  $h$ ,  $H$  and  $A$  mix at the loop level [18–21], resulting in the (mass ordered)  $h_1$ ,  $h_2$  and  $h_3$ , which are not states of definite  $\mathcal{CP}$ -parity. In the following we denote the light Higgs with  $h_1$ , independent whether the parameters are chosen complex or real. The Higgs sector predictions have been derived with `FeynHiggs 2.9.4` [22–25] (the most recent corrections to the Higgs boson masses as derived in Ref. [26] are not included, but expect to have a small impact on the parameters used here, see below).

In the limit  $\mu \gg |M_1|, M_2$ ;  $M_{H^\pm} \gg M_Z$ ;  $\tan\beta \gg 1$ , which will be relevant for most of the analyzed benchmark scenarios, we obtained simplified expressions for the couplings for  $\tilde{\chi}_i^0 \tilde{\chi}_j^0 Z/h_1$  in Ref. [16]. Here the two lightest neutralinos are almost purely bino and wino-like states,  $\tilde{\chi}_1^0 \sim \tilde{B}$ ,  $\tilde{\chi}_2^0 \sim \tilde{W}$ . For simplicity we neglect the mixing between the bino and wino components, which has a subleading effect in our approximation, such that  $N_{12} \simeq N_{21} \simeq 0$ , while  $|N_{11}| \simeq |N_{22}| \simeq 1$ . Note that in the Higgs decoupling limit [27] one has  $(\beta - \alpha) \rightarrow \pi/2$ . In this limit we obtain

$$C_{\tilde{\chi}_1^0 \tilde{\chi}_2^0 Z}^L \approx \frac{e M_Z^2}{2 \mu^2} \exp\left(\frac{i\varphi_{M_1}}{2}\right), \quad (1)$$

$$C_{\tilde{\chi}_1^0 \tilde{\chi}_2^0 h_1}^L \approx \frac{e M_Z}{2 \mu} \left( \frac{M_1 + M_2}{\mu} + \frac{4}{\tan\beta} \right) \exp\left(\frac{-i\varphi_{M_1}}{2}\right), \quad (2)$$

where the neglected terms are of higher order in  $M_Z/\mu$ ,  $M_{1/2}/\mu$  and  $1/\tan\beta$ . Here  $e$  denotes the electric charge,  $\alpha_{\text{em}} = e^2/(4\pi)$ , and  $\alpha$  is the angle that diagonalizes the  $\mathcal{CP}$ -even Higgs

sector at tree-level. From Eq. (2) it follows that the absolute value of the Higgs coupling is largest (smallest) for positive (negative)  $M_1$ . Note that the partial decay widths, for which explicit expressions can be found in Ref. [16], also depend on the relative intrinsic  $\mathcal{CP}$  of the neutralinos, and that of the Higgs or ( $\mathcal{CP}$ -even)  $Z$ -boson. Near the decay threshold this effect, which arises due to the p-wave suppression of some of the amplitudes, leads to a stronger dependence on the  $\mathcal{CP}$ -phases than the one resulting from the change in the absolute value of the couplings, provided  $m_{\tilde{\chi}_1^0} \neq 0$ , as shown in Ref. [16].

Before reviewing our results, we will first briefly describe the calculations used for the direct production cross section of  $\tilde{\chi}_2^0 \tilde{\chi}_1^\pm$ , and for the branching ratios for the subsequent decay of the neutralino into a  $Z$  boson and of the chargino into a  $W$  boson and the LSP. The production of neutralinos and charginos at the LHC is calculated using the program `Prospino 2.1` [28]. Complex parameters can only affect these cross sections when the charginos or neutralinos are mixed states, and we estimate such effects to be negligible for our set-up, so we adopt the `Prospino` results which neglect CP phases to hold. We further neglect the NLL corrections to the gaugino production cross section calculated in Ref. [29,30], estimating their effects to be at the per-cent level. For the decay widths we employ our full NLO corrections in the on-shell scheme of the complex MSSM (see e.g. [31]) as calculated in Refs. [32,33]. The calculation is based on `FeynArts/Formcalc` [34,35], and the corresponding model file conventions [36] are used throughout. The benchmark scenarios defined in the following section are such that the decays  $\tilde{\chi}_1^\pm \rightarrow \tilde{\chi}_1^0 W^\pm$  as well as  $\tilde{\chi}_2^0 \rightarrow \tilde{\chi}_1^0 Z$ ,  $\tilde{\chi}_2^0 \rightarrow \tilde{\chi}_1^0 h_1$  are the only relevant ones. As analyzed in the previous subsection the decays of a wino-like  $\tilde{\chi}_2^0$  to  $\tilde{\chi}_1^0 h_i$  are most sensitive to  $\varphi_{M_1}$  due to the relative  $\mathcal{CP}$  between the bino-like  $\tilde{\chi}_1^0$  and the wino-like  $\tilde{\chi}_2^0$ , which is controlled by  $\varphi_{M_1}$ .

## 2.2 Definition of benchmark scenarios

The baseline analysis in Ref. [16] made use of results reported by ATLAS using the full 2012 data set, where numerical values were provided for the excluded cross sections [10] (but could equally be applied on more recent Analyses, such as in Ref. [12]). In order to interpret the ATLAS exclusions in terms of the complex MSSM, we calculate the cross section in benchmark scenarios similar to those used by ATLAS, including NLO corrections as described below. We re-analyze the ATLAS 95% CL exclusion bounds in the simplified analyses in the  $m_{\tilde{\chi}_2^0} - m_{\tilde{\chi}_1^0}$  plane, taking  $M_1$  and  $M_2$  as free parameters with central values:

$$M_1 = 100 \text{ GeV and } M_2 = 250 \text{ GeV.} \quad (3)$$

The other parameters are chosen as in the ATLAS analysis presented in Ref. [10]<sup>2</sup>,

$$\mu = 1 \text{ TeV, } \tan \beta = 6, \ M_{\tilde{q}_{1,2}} = M_{\tilde{q}_3} = M_{\tilde{\ell}} = 2 \text{ TeV, } A_t = 2.8 \text{ TeV.} \quad (4)$$

$M_{\tilde{q}_{1,2}}$  denotes the diagonal soft SUSY-breaking parameter in the scalar quark mass matrices of the first and second generation, similarly  $M_{\tilde{q}_3}$  for the third generation and  $M_{\tilde{\ell}}$  for all three generations of scalar leptons. If all three mass scales are identical we also use the abbreviation  $M_{\text{SUSY}} := M_{\tilde{q}_{1,2}} = M_{\tilde{q}_3} = M_{\tilde{\ell}}$ .  $A_t$  is the trilinear coupling between stop quarks and Higgs

---

<sup>2</sup> Not all parameters are clearly defined in Ref. [10]. We select and choose our parameters to be as close to the original analysis as possible.

bosons, which is chosen to give the desired value of  $M_{h_1}$ . The other trilinear couplings, set to zero in Ref. [8, 10], we set to  $A_t$  for squarks and to zero for sleptons. Setting also the  $A_{q \neq t}$  to zero would have a minor impact on our analysis. The effect the large sfermion mass scale is a small destructive interference of the  $s$ -channel amplitude with the  $t$ -channel squark exchange. The large higgsino mass parameter  $\mu$  results in a gaugino-like pair of produced neutralino and chargino. The lightest Higgs boson mass (as calculated with `FeynHiggs 2.9.4` [22–25]) is evaluated to be  $\sim 125.5$  GeV, defining the value of  $A_t$  in Eq. (4). In order to scan the  $m_{\tilde{\chi}_2^0} - m_{\tilde{\chi}_1^0}$  plane we use the ranges

$$|M_1| = 0 \dots 200 \text{ GeV} , \quad M_2 = 100 \dots 400 \text{ GeV} \quad \text{with } |M_1| \leq M_2 . \quad (5)$$

The main aim of Ref. [16], as discussed above, was the interpretation of the ATLAS exclusion limits in several “physics motivated” benchmark scenarios. Taking the parameters in Eq. (4) as our baseline scenario, deviations are made in the following directions.

1. We take  $\varphi_{M_1}$ , the phase of  $M_1$ , to be a free parameter. Note that for the considered central benchmark scenario, as  $\tan \beta$  is low and  $M_{\text{SUSY}}$  is high, the full range is allowed by current electric dipole moment (EDM) constraints [37–39], as verified explicitly via both `CPsuperH 2.3` [40–42] and `FeynHiggs 2.9.4` [22–25].
2. The variation of  $\tan \beta$  can have a strong impact on the couplings between the neutralinos and the Higgs boson, see Eq. (2). We therefore analyze the effect of variation of  $\tan \beta$  in the range  $\tan \beta = 6 \dots 20$ .

The various scenarios are summarized in Tab. 1

Scenario	$\varphi_{M_1}$	$\mu$	$\tan \beta$	$M_{\text{SUSY}}$
$S_{\text{ATLAS}}$	0	1000	6	2000
$S_{\text{ATLAS}}^{\varphi_{M_1}}$	$0 \dots \pi$	1000	6	2000
$S_{\text{ATLAS}}^{\tan \beta}$	0	1000	$6 \dots 20$	2000

Table 1: Parameters for benchmark scenarios (masses in GeV). We furthermore have for all scenarios:  $|M_1| = 0 \dots 200$  GeV,  $M_2 = 100 \dots 400$  GeV (with  $|M_1| \leq M_2$ ),  $M_3 = 1500$  GeV (gluino mass parameter). The first (baseline) scenario corresponds to the ATLAS analysis in Ref. [10]. Our “central benchmark scenario” refers to the case  $M_1 = 100$  GeV and  $M_2 = 250$  GeV. The value of  $A_t$  is adjusted to ensure  $M_{h_1} \approx 125.5$  GeV.

## 2.3 Results

The main results are summarized in Fig. 1, where the exclusion region is shown in the  $m_{\tilde{\chi}_2^0} - m_{\tilde{\chi}_1^0}$  plane for  $\tan \beta = 6$  (upper plot) and  $\tan \beta = 20$  (lower plot). The solid lines (shaded areas) correspond to the data presented in Ref. [8]. The dashed lines are the projection for

the combination of ATLAS and CMS LHC8 data, calculated as described in Ref. [16]. The red lines show the ATLAS analysis, the green lines take into account the decays  $\tilde{\chi}_2^0 \rightarrow \tilde{\chi}_1^0 h_1$  for  $M_1 > 0$ , and the blue ones for  $M_1 < 0$ . The exclusion curves are not smooth, reflecting the fact that excluded cross sections obtained from ATLAS are only available for a sparse grid of points in the  $m_{\tilde{\chi}_2^0} - m_{\tilde{\chi}_1^0}$  plane, and are given both for the ATLAS data and for LHC8 combined data. Technically, this is achieved by interpolating the cross section as a function of  $m_{\tilde{\chi}_1^0}$  for fixed values of  $m_{\tilde{\chi}_2^0}$ . Note that above the light (dark) gray line the on-shell decay  $\tilde{\chi}_2^0 \rightarrow \tilde{\chi}_1^0 Z(h_1)$  is kinematically forbidden.

The results for scenario  $S_{\text{ATLAS}}$ , i.e. with  $\tan \beta = 6$ , are shown in the upper figure. The area excluded by ATLAS is drastically reduced when the decay  $\tilde{\chi}_2^0 \rightarrow \tilde{\chi}_1^0 h_1$  is taken into account. Only the region where  $\tilde{\chi}_2^0 \rightarrow \tilde{\chi}_1^0 h_1$  is kinematically forbidden, and a small strip close to the kinematic limit can be excluded by the current ATLAS analysis. The excluded area grows marginally taking into account the projection for the LHC8 full data set, i.e. the projected combination of ATLAS and CMS data.

We show the results for scenario  $S_{\text{ATLAS}}^{\tan \beta}$ , i.e. with  $\tan \beta = 20$ , in the lower figure of Fig. 1. While below the Higgs threshold the exclusions are independent of  $\tan \beta$ , above this threshold the excluded regions are somewhat larger for  $\tan \beta = 20$ . However, the excluded region is clearly reduced in comparison to the simplified model case where the Higgs channel is neglected. Again, Fig. 1 can easily be understood via Eqs. (1) and (2), where we see that for smaller  $\tan \beta$  and large  $\mu$  the Higgs channel dominates, and the branching ratio to the  $Z$  boson is considerably smaller than one.

As discussed in Sec. 2.1, the neutralino-Higgs coupling decreases with  $\varphi_{M_1}$ , and in Eq. (2) we see the sensitivity to the phase increases with  $\tan \beta$ . This  $\varphi_{M_1}$  dependence affects the exclusion bounds on  $M_1$  and  $M_2$ , as illustrated in Fig. 2, where we consider the ATLAS exclusion limits in the  $\varphi_{M_1} - M_1$  plane, for  $\tan \beta = 6$  (left) and 20 (right), and for  $\Delta := M_2 - M_1 = M_{h_1}, 130, 150, 180$  GeV (which defines the value of  $M_2$  in the plots). The values of  $\Delta$  here correspond approximately to diagonal lines in the  $m_{\tilde{\chi}_2^0} - m_{\tilde{\chi}_1^0}$  plane in Fig. 1, starting from the Higgs threshold at  $\Delta = M_{h_1}$ . The solid (dotted) lines indicate the calculation is at NLO (tree-level). The limits in red are given by the requirement that the EDMs for thallium and mercury,  $d_{\text{Tl}}(M_{\text{SUSY}})$  and  $d_{\text{Hg}}(M_{\text{SUSY}})$ , calculated using `CPsuperH 2.3` [40–42]<sup>3</sup> for a specific value of  $M_{\text{SUSY}}$  within  $S_{\text{ATLAS}}^{\text{SUSY}}$ , are below the upper limit, i.e.  $d_{\text{Tl}}^{\text{exp}} = 9.0 \cdot 10^{-25} e \text{ cm}$  (90% CL) or  $d_{\text{Hg}}^{\text{exp}} = 3.1 \cdot 10^{-29} e \text{ cm}$  (95% CL) [38, 39]. We adopt a common mass scale  $M_{\text{SUSY}} = M_{\tilde{q}_{1,2}} = M_{\tilde{g}_3} = M_{\tilde{\ell}}$ , although the EDMs depend mainly on  $M_{\tilde{q}_{1,2}}$  and  $M_{\tilde{\ell}_{1,2}}$ . We display the limit for the EDM that provides the strongest bound, i.e. from  $d_{\text{Tl}}$  for  $\tan \beta = 6$  and from  $d_{\text{Hg}}$  for  $\tan \beta = 20$ . Although  $M_{\text{SUSY}} = 0.8$  TeV is disfavored at the LHC, we show these limits for comparison, as there is no exclusion from the EDMs for higher values of  $M_{\text{SUSY}}$  (i.e. in  $S_{\text{ATLAS}}$ ) for  $\tan \beta = 6$ .

From Fig. 2 one can clearly see how  $\varphi_{M_1}$  affects the exclusion limit on  $M_1$ , which is much stronger for  $\varphi_{M_1} = \pi$  than for  $\varphi_{M_1} = 0$ , as also seen in Fig. 1. Furthermore, as discussed above, the effect of the phase is clearly much more pronounced at lower values of  $\tan \beta$ . On varying  $\varphi_{M_1}$  from 0 to  $\pi$ , for  $\Delta = 130$  GeV, the limit on  $M_1$  changes by  $\sim 80$  GeV for  $\tan \beta = 6$  in contrast to 50 GeV for  $\tan \beta = 20$ . Note that the exclusion disappears completely for  $\Delta > 135$  GeV for  $\tan \beta = 6$  and  $\Delta > 200$  GeV for  $\tan \beta = 20$ . The  $\Delta = M_{h_1}$

<sup>3</sup> Similar results can be obtained with `FeynHiggs` [22–25].

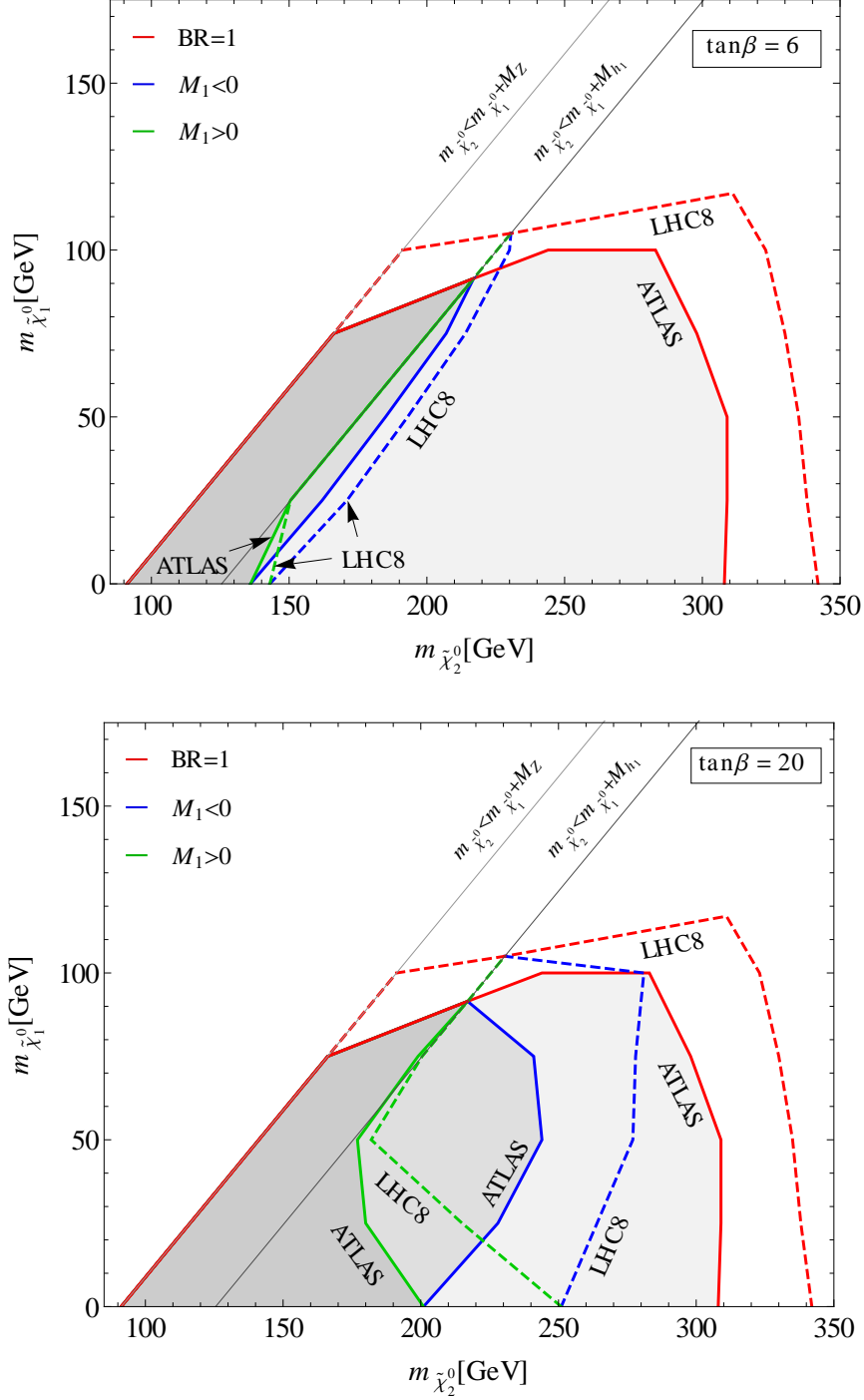


Figure 1: Contours showing the approximate excluded region from  $S_{\text{ATLAS}}$  in the  $m_{\tilde{\chi}_2^0} - m_{\tilde{\chi}_1^0}$  plane with  $\tan\beta = 6$  (upper plot) and  $\tan\beta = 20$  (lower plot). The solid lines (shaded areas) correspond to the exclusion for the analyzed ATLAS data [8], and the dashed lines indicate our projection for the combined LHC8 data, both for the case where it is assumed  $\text{BR}(\tilde{\chi}_2^0 \rightarrow \tilde{\chi}_1^0 Z) = 1$ , and where the decays  $\tilde{\chi}_2^0 \rightarrow \tilde{\chi}_1^0 h_1$  are taken into account for  $M_1 > 0$  (green), and for  $M_1 < 0$  (blue) as indicated, calculating  $\text{BR}(\tilde{\chi}_2^0 \rightarrow \tilde{\chi}_1^0 Z)$  at NLO. Above the light (dark) gray line the on-shell decay  $\tilde{\chi}_2^0 \rightarrow \tilde{\chi}_1^0 Z (h_1)$  is kinematically forbidden.

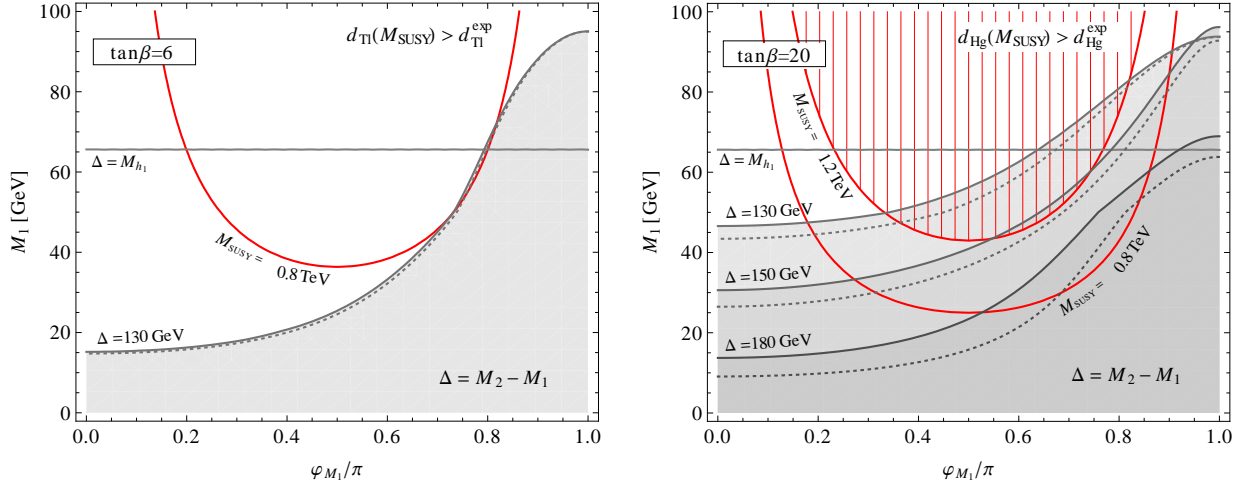


Figure 2: Contours showing the excluded region from currently analyzed ATLAS data for  $S_{\text{ATLAS}}$  in the  $M_1$ - $\varphi_{M_1}$  plane, with  $\tan\beta = 6$  (left) and  $\tan\beta = 20$  (right).  $M_2$  is fixed via  $\Delta = M_2 - M_1$ , which corresponds approximately to diagonal lines in e.g. Fig. 1, parallel to the Higgs threshold given by  $\Delta = M_{h_1}$ . The solid (dotted) lines indicate that the exclusion contours are calculated using NLO (tree-level) branching ratios for the  $\tilde{\chi}_2^0$  decays. At  $\Delta = 150$  GeV for  $\tan\beta = 6$  and  $\Delta = 210$  GeV for  $\tan\beta = 20$  there is no exclusion from ATLAS. The red lines define exclusion contours for  $S_{\text{ATLAS}}^{\text{SUSY}}$ , where  $M_{\text{SUSY}}$  is indicated (see text), from the EDMs of thallium ( $d_{\text{Tl}}$ ) and mercury ( $d_{\text{Hg}}$ ).

line is also shown in order to illustrate that below the Higgs threshold, the dependence on  $\varphi_{M_1}$  vanishes.

From the right plot of Fig. 2 we notice that the one-loop corrections, i.e. the difference between solid and dotted lines, are clearly sizeable for  $\tan\beta = 20$ , shifting the excluded value of  $M_1$  (for fixed  $\varphi_{M_1}$ ) by up to  $\sim 12$  GeV for  $\Delta = 180$  GeV.

### 3 Conclusions

We have reviewed the exclusion limits on the parameters describing the electroweak sector of the MSSM from direct  $\tilde{\chi}_1^\pm \tilde{\chi}_2^0$  production searches via  $WZ + E_T^{\text{miss}}$  at the LHC. We started by considering the baseline scenario used by ATLAS in their public note for  $21 \text{ fb}^{-1}$  [10], where it is assumed that the  $\tilde{\chi}_1^\pm$  and  $\tilde{\chi}_2^0$  decay 100% via  $\tilde{\chi}_1^\pm \rightarrow \tilde{\chi}_1^0 W^\pm$  and  $\tilde{\chi}_2^0 \rightarrow \tilde{\chi}_1^0 Z$ , and limits on  $m_{\tilde{\chi}_2^0}$  of up to  $\sim 300$  GeV are derived. We investigated how these limits are affected when using NLO results both for the SUSY production cross sections as well as for the branching ratio calculations. We found that, apart from the region where  $\tilde{\chi}_2^0 \rightarrow \tilde{\chi}_1^0 h_1$  is kinematically forbidden<sup>4</sup>, only a very small strip in the  $m_{\tilde{\chi}_2^0} - m_{\tilde{\chi}_1^0}$  plane can be excluded in this baseline scenario. Allowing the gaugino mass parameter  $M_1$  to take negative values (corresponding to  $\varphi_{M_1} = \pi$ ), slightly larger regions in the  $m_{\tilde{\chi}_2^0} - m_{\tilde{\chi}_1^0}$  plane can be excluded. Going from the

<sup>4</sup> It is interesting to note that in that region the most recent ATLAS analysis [12] found a  $\sim 1.5\sigma$  excess of events.



baseline value  $\tan\beta = 6$  to  $\tan\beta = 20$  again leads to somewhat larger excluded regions, but the decay  $\tilde{\chi}_2^0 \rightarrow \tilde{\chi}_1^0 h_1$  is still clearly seen to have a substantial effect on the limits. We furthermore reviewed the dependence of the excluded mass regions on the phase of  $M_1$ , and found a strong dependence on  $\varphi_{M_1}$ . In the future, limits on  $WZ + E_T^{\text{miss}}$  and  $Wh + E_T^{\text{miss}}$  could also be exploited as a method to constrain  $\varphi_{M_1}$ , complementary to the EDMs.

Altogether these results show, on the one hand, how important it is to look at a realistic spectrum (i.e. where the decays to a Higgs boson are not neglected), and on the other hand that dedicated searches for the  $Wh + E_T^{\text{miss}}$  channel are beneficial [43]. The results indicate that there is ample room for chargino/neutralino production at the ILC with  $\sqrt{s} \leq 1$  TeV.

## Acknowledgments

A.B. gratefully acknowledges support of the DFG through the grant SFB 676, “Particles, Strings, and the Early Universe”. The work of S.H. was partially supported by CICYT (grant FPA 2010–22163-C02-01). S.H. and F.v.d.P. were supported by the Spanish MICINN’s Consolider-Ingenio 2010 Programme under grant MultiDark CSD2009-00064. We thank the GRID computing network at IFCA for technical help with the OpenStack cloud infrastructure [44].

## References

- [1] H. Nilles, *Phys. Rept.* **110** (1984) 1;  
H. Haber and G. Kane, *Phys. Rept.* **117** (1985) 75;  
R. Barbieri, *Riv. Nuovo Cim.* **11** (1988) 1.
- [2] R. Mahbubani, M. Papucci, G. Perez, J. Ruderman and A. Weiler, *Phys. Rev. Lett.* **110** (2013) 15, 151804 [arXiv:1212.3328 [hep-ph]].
- [3] S. AbdusSalam, B. Allanach, H. Dreiner, J. Ellis, U. Ellwanger, J. Gunion, S. Heinemeyer and M. Krämer et al., *Eur. Phys. J. C* **71** (2011) 1835 [arXiv:1109.3859 [hep-ph]].
- [4] M. Benayoun, P. David, L. DelBuono and F. Jegerlehner, *Eur. Phys. J. C* **73** (2013) 2453 arXiv:1210.7184 [hep-ph].
- [5] S. Heinemeyer, W. Hollik, G. Weiglein and L. Zeune, *JHEP* **1312** (2013) 084 [arXiv:1311.1663 [hep-ph]].
- [6] K. Rolbiecki and K. Sakurai, *JHEP* **1309** (2013) 004 [arXiv:1303.5696 [hep-ph]].
- [7] G. Aad et al. [ATLAS Collaboration], *Phys. Lett. B* **718** (2013) 841 [arXiv:1208.3144 [hep-ex]].
- [8] [ATLAS Collaboration], ATLAS-CONF-2012-154.
- [9] [ATLAS Collaboration], ATLAS-CONF-2013-028.
- [10] [ATLAS Collaboration], ATLAS-CONF-2013-035.

- [11] [ATLAS Collaboration], ATLAS-CONF-2013-049.
- [12] G. Aad *et al.* [ATLAS Collaboration], arXiv:1403.5294 [hep-ex].
- [13] S. Chatrchyan *et al.* [CMS Collaboration], *JHEP* **1211** (2012) 147 [arXiv:1209.6620 [hep-ex]].
- [14] S. Chatrchyan *et al.* [CMS Collaboration], CMS PAS SUS-12-022.
- [15] A. Bharucha, J. Kalinowski, G. Moortgat-Pick, K. Rolbiecki and G. Weiglein, *Eur. Phys. J. C* **73** (2013) 2446 [arXiv:1211.3745 [hep-ph]].
- [16] A. Bharucha, S. Heinemeyer and F. von der Pahlen, *Eur. Phys. J. C* **73** (2013) 2629 [arXiv:1307.4237 [hep-ph]].
- [17] V. Barger, T. Falk, T. Han, J. Jiang, T. Li and T. Plehn, *Phys. Rev. D* **64** (2001) 056007 [arXiv:hep-ph/0101106].
- [18] A. Pilaftsis, *Phys. Rev. D* **58** (1998) 096010 [arXiv:hep-ph/9803297];  
A. Pilaftsis, *Phys. Lett. B* **435** (1998) 88 [arXiv:hep-ph/9805373].
- [19] D. Demir, *Phys. Rev. D* **60** (1999) 055006 [arXiv:hep-ph/9901389].
- [20] A. Pilaftsis and C. Wagner, *Nucl. Phys. B* **553** (1999) 3 [arXiv:hep-ph/9902371].
- [21] S. Heinemeyer, *Eur. Phys. J. C* **22** (2001) 521 [arXiv:hep-ph/0108059].
- [22] S. Heinemeyer, W. Hollik and G. Weiglein, *Comput. Phys. Commun.* **124** (2000) 76 [arXiv:hep-ph/9812320];  
T. Hahn, S. Heinemeyer, W. Hollik, H. Rzehak and G. Weiglein, *Comput. Phys. Commun.* **180** (2009) 1426; see [www.feynhiggs.de](http://www.feynhiggs.de).
- [23] S. Heinemeyer, W. Hollik and G. Weiglein, *Eur. Phys. J. C* **9** (1999) 343 [arXiv:hep-ph/9812472].
- [24] G. Degrandi, S. Heinemeyer, W. Hollik, P. Slavich and G. Weiglein, *Eur. Phys. J. C* **28** (2003) 133 [arXiv:hep-ph/0212020].
- [25] M. Frank, T. Hahn, S. Heinemeyer, W. Hollik, R. Rzehak and G. Weiglein, *JHEP* **0702** (2007) 047 [arXiv:hep-ph/0611326].
- [26] T. Hahn, S. Heinemeyer, W. Hollik, H. Rzehak and G. Weiglein, arXiv:1312.4937 [hep-ph].
- [27] A. Dobado, M. Herrero and S. Peñaranda, *Eur. Phys. J. C* **17** (2000) 487 [arXiv:hep-ph/0002134];  
J. Gunion and H. Haber, *Phys. Rev. D* **67** (1993) 075019 [arXiv:hep-ph/0207010];  
H. Haber and Y. Nir, *Phys. Lett. B* **306** (1993) 327 [arXiv:hep-ph/9302228];  
H. Haber, arXiv:hep-ph/9505240.

- [28] W. Beenakker, M. Klasen, M. Kramer, T. Plehn, M. Spira and P. Zerwas, *Phys. Rev. Lett.* **83** (1999) 3780 [Erratum-ibid. **100** (2008) 029901] [arXiv:hep-ph/9906298].
- [29] B. Fuks, M. Klasen, D. R. Lamprea and M. Rothering, *JHEP* **1210** (2012) 081 [arXiv:1207.2159 [hep-ph]].
- [30] B. Fuks, M. Klasen, D. R. Lamprea and M. Rothering, *Eur. Phys. J. C* **73** (2013) 2480 [arXiv:1304.0790 [hep-ph]].
- [31] A. Bharucha, A. Fowler, G. Moortgat-Pick and G. Weiglein, *JHEP* **1305** (2013) 053 [arXiv:1211.3134 [hep-ph]].
- [32] S. Heinemeyer, F. von der Pahlen and C. Schappacher, *Eur. Phys. J. C* **72** (2012) 1892 [arXiv:1112.0760 [hep-ph]].
- [33] A. Bharucha, S. Heinemeyer, F. von der Pahlen and C. Schappacher, *Phys. Rev. D* **86** (2012) 075023 [arXiv:1208.4106 [hep-ph]].
- [34] J. Küblbeck, M. Böhm and A. Denner, *Comput. Phys. Commun.* **60** (1990) 165; T. Hahn, *Comput. Phys. Commun.* **140** (2001) 418 [arXiv:hep-ph/0012260]; T. Hahn and C. Schappacher, *Comput. Phys. Commun.* **143** (2002) 54 [arXiv:hep-ph/0105349].  
The program, the user's guide and the MSSM model files are available via [www.feynarts.de](http://www.feynarts.de).
- [35] T. Hahn and M. Pérez-Victoria, *Comput. Phys. Commun.* **118** (1999) 153 [arXiv:hep-ph/9807565].
- [36] T. Fritzsche, T. Hahn, S. Heinemeyer, F. von der Pahlen, H. Rzehak and C. Schappacher, arXiv:1309.1692 [hep-ph];  
The couplings can be found in the files `MSSM.ps.gz`, `MSSMQCD.ps.gz` and `HMix.ps.gz` as part of the `FeynArts` package [34].
- [37] C. Baker et al., *Phys. Rev. Lett.* **97** (2006) 131801 [arXiv:hep-ex/0602020].
- [38] B. Regan, E. Commins, C. Schmidt and D. DeMille, *Phys. Rev. Lett.* **88** (2002) 071805.
- [39] W. Griffith, M. Swallows, T. Loftus, M. Romalis, B. Heckel and E. Fortson, *Phys. Rev. Lett.* **102** (2009) 101601.
- [40] J. Lee, M. Carena, J. Ellis, A. Pilaftsis and C. Wagner, *Comput. Phys. Commun.* **184** (2013) 1220 [arXiv:1208.2212 [hep-ph]].
- [41] J. Lee, M. Carena, J. Ellis, A. Pilaftsis and C. Wagner, *Comput. Phys. Commun.* **180** (2009) 312 [arXiv:0712.2360 [hep-ph]].
- [42] J. Lee, A. Pilaftsis, M. Carena, S. Choi, M. Drees, J. Ellis and C. Wagner, *Comput. Phys. Commun.* **156** (2004) 283 [arXiv:hep-ph/0307377].

- [43] H. Baer, V. Barger, A. Lessa, W. Sreethawong and X. Tata, *Phys. Rev. D* **85** (2012) 055022 [arXiv:1201.2949 [hep-ph]].
- [44] I. Campos, E. del Castillo, S. Heinemeyer, A. Lopez-Garcia and F. von der Pahlen, *Eur. Phys. J. C* **73** (2013) 2375 [arXiv:1212.4784 [cs.DC]].